AD-A165 605 THE INFRARED MULTIPHOTON DISSOCIATION OF THREE NITROLKANES(U) CALIFORNIA UNIV BERKELEY DEPT OF CHEMISTRY A M WODTKE ET AL. 24 JAN 86 N00014-83-K-0069 1/1

UNCLASSIFIED F/G 7/4 NL

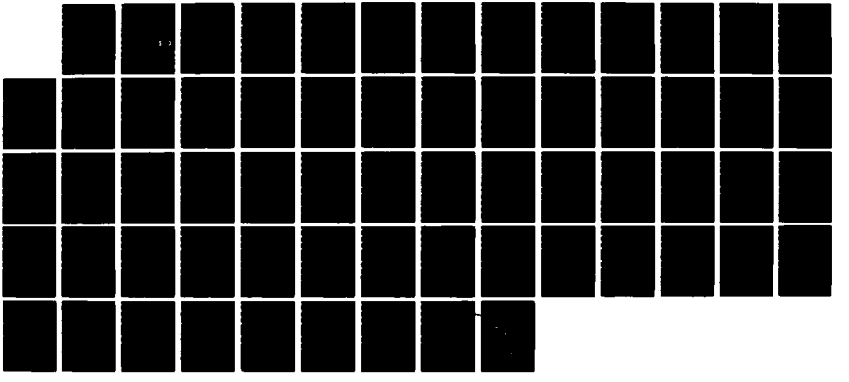

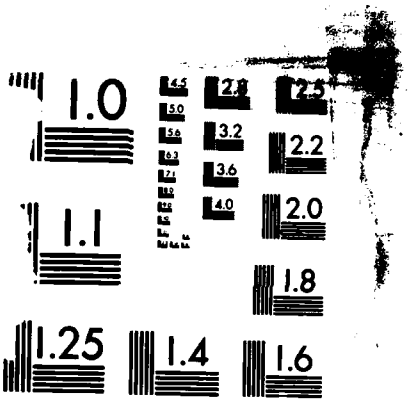

(12)

SECURITY CLASSIFICATION OF THIS PAGE (When Data Entered)

REPORT DOCUMENTATION PAGE		READ INSTRUCTIONS BEFORE COMPLETING FORM
1. REPORT NUMBER NR 659-819/1/86	2. GOVT ACCESSION NO.	3. RECIPIENT'S CATALOG NUMBER
4. TITLE (and Subtitle) THE INFRARED MULTIPHOTON DISSOCIATION OF THREE NITROLKANES		5. TYPE OF REPORT & PERIOD COVERED TECHNICAL 6. PERFORMING ORG. REPORT NUMBER
7. AUTHOR(s) A. M. Wodtke, E. J. Hintsa, and Y. T. Lee		8. CONTRACT OR GRANT NUMBER(s) N00014-83-K-0069 NR 659-819
9. PERFORMING ORGANIZATION NAME AND ADDRESS Professor Yuan T. Lee Dept. of Chemistry, Univ. of California Berkeley, CA 94720		10. PROGRAM ELEMENT, PROJECT, TASK AREA & WORK UNIT NUMBERS
11. CONTROLLING OFFICE NAME AND ADDRESS Dr. Richard S. Miller, Office of Naval Research Department of the Navy, Code 432P 800 N. Quincy Street, Arlington, VA 22217		12. REPORT DATE January 24, 1986 13. NUMBER OF PAGES 60
14. MONITORING AGENCY NAME & ADDRESS(if different from Controlling Office) Office of Naval Research Resident Representative UCB Residency, Richmond Field Station Univ. of Calif., Berkeley, CA 94720		15. SECURITY CLASS. (of this report) UNCLASSIFIED 15a. DECLASSIFICATION/DOWNGRADING SCHEDULE

16. DISTRIBUTION STATEMENT (of this Report)

Unlimited

This document has been approved for public release and sale; its distribution is unlimited.

DTIC ELECTE MAR 19 1986 S D

17. DISTRIBUTION STATEMENT (of the abstract entered in Block 20, if different from Report)

18. SUPPLEMENTARY NOTES

None

19. KEY WORDS (Continue on reverse side if necessary and identify by block number)

Unimolecular decomposition; thermal chemistry; IRMPD; nitroalkanes; molecular beams; concerted molecular elimination; RRKM theory.

20. ABSTRACT (Continue on reverse side if necessary and identify by block number)

(See reverse side)

DD FORM 1 JAN 73 1473 EDITION OF 1 NOV 65 IS OBSOLETE
S/N 0102-LF-014-6601

SECURITY CLASSIFICATION OF THIS PAGE (When Data Entered)

20. Abstract

Infrared multiphoton dissociation in a molecular beam has been studied in order to elucidate the collision free, "thermal" chemistry and dynamics of nitromethane, nitroethane and 2-nitropropane. The isomerization of CH_3NO_2 to CH_3ONO was observed by detecting the CH_3O and NO products from the dissociation of the very internally hot, isomerized nitromethane. A novel application of RRKM theory was used to estimate the barrier height to isomerization at 55.5 kcal/mol. The barrier height determination method was tested and found to give excellent results by applying it to the determination of the barrier height to HONO elimination from nitroethane, a value which is well known from activation energy measurements. The method was then applied to the case of HONO elimination from 2-nitropropane and it appears that there is good reason to believe that the barrier height is 3-5 kcal/mol lower in 2-nitropropane than in nitroethane. The success of this method for determining barrier heights shows how a "microscopic" molecular beam experiment, using infrared multiphoton dissociation where the concept of temperature has no place, can be quantitatively related to pyrolysis experiments which are conducted under collisional, thermal conditions and measure phenomenological quantities such as activation energies. The concerted HONO elimination reactions from nitroethane and 2-nitropropane were found to channel about 70 and 65 percent of the exit barrier into translation, respectively. This large release of translational energy is suggested to be due to the nature of the transition state mechanical barrier which is largely made up of repulsive energy between the closed shell products and not of reactant strain energy. The small difference between nitroethane and 2-nitropropane in the translational energy distributions is explained in terms of a scaled reduced mass impulse approximation that is used to characterize the repulsive excitation dynamics of the departing closed shell products.

THE INFRARED MULTIPHOTON DISSOCIATION OF THREE NITROALKANES

A. M. Wodtke, E. J. Hintsa, and Y. T. Lee

Materials and Molecular Research Division
Lawrence Berkeley Laboratory and
Department of Chemistry, University of California
Berkeley, California 94720 USA

ABSTRACT

Infrared multiphoton dissociation in a molecular beam has been studied in order to elucidate the collision free, "thermal" chemistry and dynamics of nitromethane, nitroethane and 2-nitropropane. The isomerization of CH_3NO_2 to CH_3ONO was observed by detecting the CH_3O and NO products from the dissociation of the very internally hot, isomerized nitromethane. A novel application of RRKM theory was used to estimate the barrier height to isomerization at 55.5 kcal/mol. The barrier height determination method was tested and found to give excellent results by applying it to the determination of the barrier height to HONO elimination from nitroethane, a value which is well known from activation energy measurements. The method was then applied to the case of HONO elimination from 2-nitropropane and it appears that there is good reason to believe that the barrier height is 3-5 kcal/mol lower in 2-nitropropane than in nitroethane. The success of this method for determining barrier heights shows how a "microscopic" molecular beam experiment, using infrared multiphoton dissociation where the concept of temperature has no place, can be quantitatively related to pyrolysis experiments which are conducted under collisional, thermal conditions and measure phenomenological quantities such as activation energies. The

concerted HONO elimination reactions from nitroethane and 2-nitropropane were found to channel about 70 and 65 percent of the exit barrier into translation, respectively. This large release of translational energy is suggested to be due to the nature of the transition state mechanical barrier which is largely made up of repulsive energy between the closed shell products and not of reactant strain energy. The small difference between nitroethane and 2-nitropropane in the translational energy distributions is explained in terms of a scaled reduced mass impulse approximation that is used to characterize the repulsive excitation dynamics of the departing closed shell products.

THE INFRARED MULTIPHOTON DISSOCIATION OF THREE NITROALKANES

I. INTRODUCTION

The discovery of infra-red, multiple-photon absorption (IRMPA) and dissociation (IRMPD) in isolated polyatomic molecules raised great hopes that one could direct chemical reactions, since IRMPA allows one to put a great deal of energy directly into the nuclear motion of a polyatomic molecule through a specific vibrational degree of freedom.[1-5] The subsequent discovery that IRMPD could be isotopically selective,[6-8] aroused continued enthusiasm among some scientists about the possibilities of bond selective chemistry. A plethora of review articles has appeared on these and related topics.[9] It is now generally realized that the quest for mode specific chemistry by IRMPD is not technologically possible because of very fast intramolecular vibrational redistribution (IVR) in highly vibrationally excited polyatomic molecules. Several experiments have shown that this typically occurs on a picosecond time scale or faster.[10,11] The profound implications of this can be appreciated if one realizes that even for strong IR absorbers ($\sigma = 10^{-17}$ cm^2) and intense IR sources (I = 10^{26} photons cm^{-2} sec^{-1}), the average time it takes to absorb a single photon is 10^{-9} sec.

In spite of the "problem" of picosecond IVR, in fact because of it, there are certain advantages to studying the dissociation of polyatomic molecules by IRMPD. The first of these is that statistical theories of unimolecular decomposition[12] which assume the free flow of vibrational

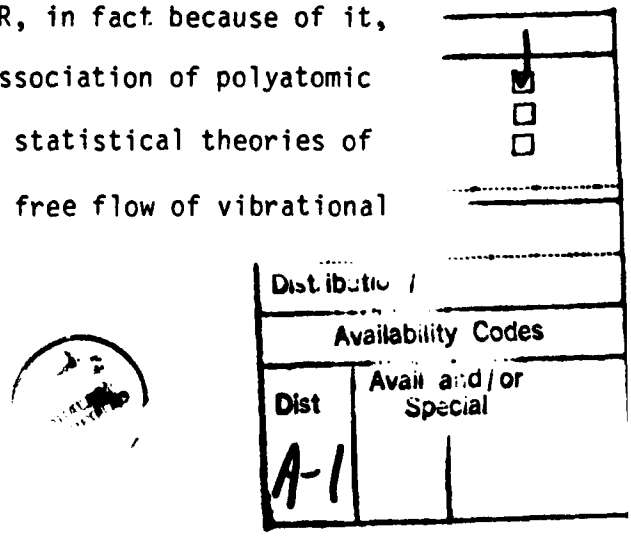

energy in the dissociating molecule can be used to describe the dissociation process and thus interpret experimental results. The validity and usefulness of various statistical theories, especially the most commonly used RRKM theory, have been widely documented in the literature.[13-18]

The second advantage to studying IRMPD stems from the usefulness of IRMPA to "thermally heat" isolated molecules. This can be done either at low pressure in a gas cell or in the collision free environment of a molecular beam. While it is true, as has been pointed out, that IRMPA does not give rise to a vibrational population distribution that can be characterized by a temperature,[19] the difference between the population distribution created by IRMPA and that created by true thermal heating is not substantial. It has been shown that a coupled set of differential rate equations can be solved to quantitatively determine these IRMPA induced "thermal" distributions of <u>total</u> vibrational energy based on IR absorption cross sections as a function of vibrational energy.[19] This offers the very intriguing possibility of quantitatively accounting for the differences between thermal, collisional experiments which measure phenomenological quantities such as activation energies and IRMPD, molecular beam experiments which measure microscopic quantities such as potential energy barriers and do not use the concept of temperature.

One important class of reactions where RRKM theory cannot be used to predict product energy distributions is that of concerted molecular elimination reactions.[20] In this case the transition state is generally at the top of a substantial, mechanical barrier in the potential energy surface (PES). The detailed dynamics which occur as the reaction proceeds

down the exit barrier must be taken into consideration if one wishes to understand the product energy distribution. In general, a large fraction of the exit barrier is converted into product kinetic energy and the translational energy distribution peaks well away from zero, in contrast to simple bond rupture reactions with no exit barrier, whose translational energy distributions typically peak at zero. Consequently, the presence of an exit barrier in the PES can be easily determined by a direct measurement of the product translational energy distribution.

In this paper we will present an application of some of these ideas to the understanding of the energetics and dynamics of the competition between two decay channels in three prototypical nitro-compounds. In these molecules simple bond rupture competes with isomerization or concerted dissociation. Because RRKM theory can predict the translational energy distribution for simple bond rupture reactions based on the internal energy of the dissociating molecules, we can use the measured translational energy distributions for simple bond rupture reactions as a "thermometer" to derive information on the average level of internal excitation in the dissociating molecules. With this information the potential energy barrier for isomerization or concerted dissociation can be obtained based on the measured branching ratio of the two dissociation channels.

Three nitroalkanes: nitromethane (CH_3NO_2), nitroethane ($C_2H_5NO_2$) and 2-nitropropane ($CH_3CHNO_2CH_3$) have been investigated in the collision free environment of a molecular beam. The work on nitromethane has been reported cursorily before.[21] We were interested to see if there was any validity to the suggestion of an exit

barrier for simple C-N bond rupture.[22] In addition, we wanted to look for the isomerization channel to methylnitrite, CH_3ONO, and subsequent dissociation to CH_3O and NO that had been predicted theoretically.[23,24] With the application of RRKM theory, a branching ratio measurement between simple bond rupture and isomerization would then provide information upon which a good estimation of the barrier height to isomerization could be made.

Our interest in nitroethane and 2-nitropropane was due to the fact that in these two systems simple bond rupture and concerted molecular elimination occur competitively. This allows us to study the translational energy release for concerted molecular elimination reactions through a five membered ring transition state. The nitroethane experiment also provided us with a way to test the reliability of our branching ratio matching approach to the determination of the barrier height to isomerization in nitromethane, since the method can easily be applied to the determination of the barrier height to concerted molecular elimination in nitroethane, a quantity that is quite well known from activation energy measurements.

II. EXPERIMENTAL

The experimental apparatus is identical to that described previously[25], with the exception of an extra detector collimation slit used in this experiment (see below), and the use of a pulsed CO_2 laser instead of an excimer laser for excitation.

One of the aims of our experiment is to determine the probability distribution of the product's relative translational energy or $P(E_T)$ for each channel. We accomplish this by measuring the laboratory-frame, time-of-flight (TOF) "spectrum" for one or both of the recoiling fragments. Specifically, we measure the time it takes for one of the recoiling fragments to travel from the point where the laser crosses the molecular beam to the point where it is detected. The flight length is calibrated and measures 36.75 cm. The neutral products are detected by using a quadrupole-equipped mass spectrometer with electron-impact ionization and ion counting. The velocity distributions of the molecular beams of parent molecules were also analyzed by the time-of-flight method using a slotted disk spinning wheel. The experimental conditions for the three parent molecular beams used in this study are shown in table I.

The laser used in these experiment was a GENTEC, TEA, pulsed CO_2 laser operating on the R(20) line of the 9.6 μm branch. Typically, the laser emmited 200 mJ/pulse of unpolarized light at 35 Hz and the output was focussed down to a 0.06 cm diameter circular spot to give a laser fluence of ~75 J/cm^2. The laser pulse had the characteristic 200 nsec "spike" of IR emmission followed by a 600 nsec tail.

Due to the low translational energy release in many of the reactions studied in these experiments it was neccesary to obtain data close to the molecular beam. Therefore all of the data were taken at 10° from the molecular beam. In order to lower the background which at this angle mainly originates from effusion at the second skimmer of the molecular beam source, an extra defining slit (circular, 0.4 cm dia.) was placed 3.81 cm from the

interaction region, between the interaction region and the detector. This had the effect of cutting out 80 percent of the background without losing any signal by limiting the viewing window of the detector to the minimum neccesary to "see" the entire interaction region.

The chemicals used in these experiments were commercially obtained and used without purification.

III. RESULTS AND DATA ANALYSIS

The data in this experiment appear in three forms. First, the mass spectra of the laser induced dissociation products contain information on the identity of the collision free dissociation pathways. Second, the intensities of the signal at each mass (actually m/e) yield information on the branching ratio's of competing dissociation channels. Third, the TOF spectrum for each mass is reflective of the translational energy distribution of the products of each channel. Although we normally measure the TOF spectra of both recoiling fragments of a given dissociation channel, in principle this is not necessary since in the center-of-mass (c.m.) frame, the velocity of the second fragment can be obtained from the first by conservation of linear momentum. In practice, because we do measure the TOF spectra of each fragment we can use the conservation of linear momentum to unambiguously determine which products belong to the same dissociation channel in complex reaction systems with more than one important decomposition pathway. This is extremely important when dissocation products do not yield parent ions due to fragmentation in the ionizer.

The transformation from the lab frame to the c.m. frame was accomplished using a forward convolution method which has been described previously.[25] This method of transformation has the advantage of being able to very accurately calculate the broadening effects introduced by the experimental apparatus due to such things as the velocity spread and spatial width of the molecular beam, the finite length of the ionizer and the like. The computer program used for this data analysis takes an input $P(E_T)$ and convolutes it over the widths of the various experimental parameters. By comparing the resulting, calculated TOF to the observed TOF and by adjusting the $P(E_T)$ to obtain a good fit to the data, the c.m. frame $P(E_T)$ is derived.

A. $\underline{CH_3NO_2}$

Table II lists the IRMPD mass spectrum of nitromethane. Signal was observed at m/e = 46, 30, 29, 15. The TOF spectrum of m/e=46 (NO_2^+), shown in fig. 1a, is from NO_2 produced in reaction I.

$$CH_3NO_2 \xrightarrow{nh\nu} CH_3NO_2^{\ddagger} \longrightarrow CH_3 + NO_2 \qquad (I)$$

The TOF spectrum for m/e=15 (CH_3^+) which is from CH_3 radical product in reaction I is shown in fig 1b.

The solid lines drawn through the m/e=46 and 15 TOF spectra are both calculated from the $P(E_T)$ for reaction I shown in fig. 2 which is characteristic of the translational energy distribution of a simple bond rupture reaction with no exit barrier, that is, it peaks at zero and releases only a small amount of average translational energy. The arrows in

the TOF spectra mark the expected arrival time of the parent molecules if they were to travel in the same direction as the products. The small release of translational energy is indicated by the closeness of the observed TOF signal to the arrow. Because of the nature of electron-impact ionization, there will be substantial fragmentation of the NO_2 to NO^+ which should be detectable at m/e=30. The m/e=30 TOF spectrum is shown in fig 1c. The dashed curve shows the contribution to this TOF spectrum from NO_2 which fragments to NO^+ in the ionizer, calculated from the $P(E_T)$ in fig. 2. Careful inspection of the experimental data reveals that while the falling edge of the TOF spectrum is accurately simulated by the dashed curve in fig. 1c, there is an indication of substantial signal coming faster than the dashed curve which cannot be explained by reaction I alone. This is not at all surprising because the observation of a second reaction channel yielding m/e=29 (HCO^+), shown in fig. 1d, which cannot be formed by any of the products of reaction I, implies that there is a second source of NO^+. Recently it has been suggested that the barrier to isomerization of nitromethane to methylnitrite (CH_3ONO) may be low enough to compete with reaction I.[23,24] Due to the fact that the endoergicity of CH_3O + NO formation is lower than the barrier height to isomerization (see section IV. A.), isomerized CH_3ONO should contain enough internal energy to dissociate and manifest itself as production of NO (which would appear at m/e=30) and CH_3O (which would appear at m/e=30 and 29), which is exactly what has been observed.

$$CH_3NO_2^{\ddagger} \longrightarrow CH_3ONO^{\ddagger} \longrightarrow CH_3O + NO \qquad (II)$$

If we are observing CH_3O product, one might expect signal at m/e=31

(CH_3O^+). However, because electron impact ionization produces ions that are, at least initially, in the same geometrical configuration as the neutrals, i.e. a vertical transition, CH_3O^+ (methoxy cation) produced by electron impact ionization is not stable and will spontaneously decompose to form HCO^+ and H_2. The most stable form of the ion with the chemical formula CH_3O^+ is protonated formaldehyde (H_2COH^+) and not methoxy cation.[26] If reaction II is occurring, the fast part of the m/e=30 TOF spectrum that cannot be fit with reaction I alone must be momentum-matched in the c.m. coordinate system to the m/e=29 TOF spectrum through the mass ratio of the products of reaction II. By using the $P(E_T)$ shown in fig. 3 which releases somewhat more translational energy than the one for reaction I, it is possible to calculate the dashed-dot curve in the m/e=30 TOF spectrum and the solid line in the m/e=29 TOF spectrum. The $P(E_T)$ for formation of CH_3O and NO should peak at zero for the same reason that the $P(E_T)$ for the IRMPD of CH_3ONO would. This and the resulting good fit to the data confirm the existence of reaction II.

We obtain the branching ratio of reaction II to reaction I by comparing the amount of NO_2 to NO formed, measured at m/e=30. The expression for the branching ratio is shown by equation (1) which contains the proper transformation Jacobian between the lab frame and the c.m. frame for isotropic product angular distributions. Such distributions would be expected for IRMPD in which an unpolarized laser is used.

$$R = \frac{N_{NO^+/NO}(t,10^\circ)\ \sigma_{ion}(NO_2)\ F(NO^+/NO_2)\ (31)(46)}{N_{NO^+/NO_2}(t,10^\circ)\ \sigma_{ion}(NO)\ F(NO^+/NO)\ \ (15)(30)} \frac{\int P_I(E_T)\ \frac{v_{NO_2}}{u_{NO_2}}\ dv_{NO_2}}{\int P_{II}(E_T)\ \frac{v_{NO}}{u_{NO}}\ dv_{NO}} \quad (1)$$

where:

R = Branching ratio (Reaction II/Reaction I)

t = flight time of product from the point of irradiation to the detector.

$N_{NO^+/NO_x}(t,\theta)$ = TOF signal (number density of NO_x) appearing as NO^+ at time t, at a detector angle θ measured from the direction of the beam.

$\sigma_{ion}(NO_x)$ = electron impact ionization cross section for NO_x.

$F(NO^+/NO_x)$ = fraction of NO_x that fragments to NO^+ in the ionizer.

v_{NO_x} = lab frame velocity of NO_x.

u_{NO_x} = c.m. frame velocity of NO_x.

The ionization cross sections used in this calculation are derived from the empirical formula of Center and Mandl.[27]

$$\sigma_{ion} = [36(\alpha)^{0.5} - 18]\ \text{Å}^2 \qquad (2)$$

where α is the molecular polarizability in Å^3

By plugging in the measured values and performing the indicated integrals, a branching ratio of 0.6 in favor of reaction I is obtained. In this calculation, the fraction of the fast component of mass 30 that is NO^+, as opposed to CH_2O^+ is calculated to be 0.41 by requiring that in the c.m. frame, the sum of the mass 29 signal and the part of the fast contribution to mass 30 that is CH_2O^+ must equal the amount of the fast contribution to mass 30 that is NO^+ when corrected for ionization cross sections. In other words, it is required that for each NO molecule that is formed there must be one CH_3O molecule and it is assumed that ions from CH_3O only appear at masses 29 and 30.

B. $\underline{C_2H_5NO_2}$

Table III shows the IRMPD mass spectrum of nitroethane. Signal was observed at m/e = 46, 30, 29, 28, 27, and 26. The TOF spectra for these masses are shown in fig. 4a-e. The m/e=28 spectrum is not shown since, due to the large background in the detector at this mass it is impossible to obtain any useful information from this TOF spectrum. Fig. 4a shows the m/e=46 (NO_2^+) TOF spectrum and, analagously to the nitromethane case, is unambiguous evidence for the C-N bond rupture channel in the collision free unimolecular decomposition of nitroethane. The $P(E_T)$ for reaction III shown in fig. 5 generates the solid lines shown in the m/e=46 (NO_2) and m/e=29 (C_2H_5) TOF spectra.

$$C_2H_5NO_2 \xrightarrow{nh\nu} C_2H_5NO_2^{\ddagger} \longrightarrow C_2H_5 + NO_2 \qquad \text{(III)}$$

Further verification of this assignment is given by the fact that the slow part of the m/e=30 TOF spectrum (shown as the dashed curve) is fit simply assuming fragmentation in the ionizer of NO_2 to NO^+. Similarly, the slow parts of the m/e=27 and 26 TOF spectra (shown as dashed curves) are based on the fragmentation in the ionizer of ethyl radical to these masses.

One can see from the m/e=30, 27 and 26 TOF spectra that there is also a second reaction channel appearing which is releasing a much larger amount of translational energy than reaction III. It is known from thermal decomposition studies that reaction IV is a low energy decomposition pathway.[28]

$$C_2H_5NO_2 \longrightarrow C_2H_4 + HONO \qquad \text{(IV)}$$

This reaction occurs through a five-membered cyclic transition state and forms products which are substantially more stable than the radical products of reaction III. The known activation energy is 45 kcal/mol.[28] Comparing this to an endothermicity of 18 kcal/mol, it is clear that the PES must have a substantial exit barrier. Therefore, it is not surprising that the products of reaction IV should be formed with qualitatively more translational energy than the products of reaction III. The TOF spectra of the fast products can be fit by a single $P(E_T)$ shown in fig. 6, assuming reaction IV to be their source. This argument is based on the assumption that ethyl radical appears at m/e = 29, 28, 27, 26; that ethylene appears at 28, 27, 26 and that HONO is observed only at 30. While it is clear that the observed mass spectra of ethyl radical and ethylene are reasonable, as far as we can tell, the mass spectrum of HONO has never been measured. By comparison with the mass spectrum of methylnitrite (the methyl ester of HONO), which gives no parent or mass 46,[29] it seems reasonable that HONO also should appear mainly at m/e=30.

The branching ratio between reactions III and IV can be calculated in the same way as was done above for nitromethane based on analysis of the m/e=30 TOF spectrum. The derived branching ratio of reaction IV to reaction III is 0.5 in favor of C-N bond rupture.

C. $\underline{2\text{-}C_3H_7NO_2}$

The IRMPD mass spectrum of 2-nitropropane is shown in table IV. The data is completely analagous to the nitroethane system. There is clear evidence for the simple bond rupture reaction V

$$CH_3\overset{NO_2}{\underset{|}{C}}HCH_3 \xrightarrow{nh\nu} CH_3\overset{NO_2^{\ddagger}}{\underset{|}{C}}HCH_3 \longrightarrow CH_3CHCH_3 + NO_2 \qquad (V)$$

in the m/e=46 (NO_2) TOF spectrum shown in fig. 7a which is momentum matched in the c.m. frame to the m/e=43 (2-propyl radical) TOF spectrum shown in fig. 7b. Both of these TOF spectra are fit by the $P(E_T)$ shown in fig. 8. The m/e=41 TOF spectrum shown in fig 7c, and the m/e=30 TOF spectrum shown in fig 7d both show products which are appearing with a great deal of translational energy release, and it is clear that this is evidence for HONO elimination in 2-nitropropane, exactly as in nitroethane.

$$CH_3\overset{NO_2}{\underset{|}{C}}H\,CH_3 \xrightarrow{nh\nu} CH_3\overset{NO_2^{\ddagger}}{\underset{|}{C}}H\,CH_3 \longrightarrow CH_2{=}CH{-}CH_3 + HONO \qquad (VI)$$

The $P(E_T)$ for reaction VI is shown in fig. 9.

The branching ratio between reaction V and reaction VI can be found by comparing the amount of NO_2 formed to the amount of HONO that is formed just as in the case of nitroethane. This can be done by analysis of the mass 30 TOF spectrum, the fast component of which is due to HONO and the slow component of which is due to NO_2. By knowing the fragmentation pattern of NO_2, which we measured, and by using equations 1 and 2 (see above) we arrive at a branching ratio of 0.5 in favor of simple C-N bond rupture.

IV. DISCUSSION

Because of the ability of RRKM theory to calculate both internal and translational energy distributions of products from simple bond rupture reactions without exit channel potential energy barriers,[30] given the total internal energy of the dissociating parent, we can use measured translational energy release distributions of simple bond rupture reactions in conjunction with RRKM theory to work backward and obtain information on the level of internal excitation in the dissociating parent molecule. Of course, in an IRMPD experiment the measured translational energy release distribution is the result of parent molecules dissociating with a range of internal energies, determined by the competition between photon absorption, stimulated emission and dissociation of excited molecules. In order to treat this problem in an adequate way, it is necessary to model the competing rate processes in detail. We first calculate the simple bond rupture product yield probability distribution as a function of the level of excitation of the dissociating molecules by using a computer program which solves the system of coupled differential rate equations which governs the IRMPD process. We then combine these results with RRKM theory which calculates the translational energy distributions of products dissociating from various levels of excitation. Calculating the weighted average over the product yield distribution of the RRKM $P(E_T)$'s gives a result that can be compared to experiment.[31]

In order to do this one must know the dissociation rate constants for levels above the dissociation limit. The technique for obtaining these values from RRKM theory has been discussed many times previously.[32] Briefly, the vibrational frequencies of the critical configuration are adjusted until they reproduce an accurate experimental Arrhenius A-factor. Once the frequencies of the critical configuration have been found it is easy to calculate the rate constant as a function of excitation above the dissociation limit. Because of the insensitivity of RRKM theory to the exact choice of frequencies of the critical configuration within the constraint of the A factor, rate constants derived in this way are accurate to within 10 percent.

One must also know the absorption cross sections of states in the quasicontinuum (QC) to treat this dynamic problem. In the past this has been modeled as an exponentially decreasing function of the total energy varying typically by a factor of two over the QC, but we have found empirically that for the practical purpose of determining barrier heights from an estimation of the internal energy distributions which are consistent with experimental translational energy distributions, it makes no difference if one simply lets all of the levels of the QC have the same absorption cross section. The subsequent calculation involves varying the absorption cross section for the states in the QC until the calculated internal energy distribution gives a $P(E_T)$ for simple bond rupture that agrees with the experimental data. If, for a given laser intensity,the absorption cross sections are large, there will be a greater amount of up-pumping and on the average molecules will dissociate with a larger translational energy

release. Conversely, if the absorption cross sections are small there will be on the average less up-pumping and molecules will dissociate with less energy available to translation. From the comparison of measured translational energies and model calculations the simple bond rupture channel can be used as a "thermometer" which reflects the internal energy distribution of the dissociating ensemble of molecules.

A. CH_3NO_2, BARRIER FOR ISOMERIZATION TO CH_3ONO

The estimation of the internal energy distribution is somewhat more complicated when there are competing channels of dissociation. This is shown schematically for CH_3NO_2 in fig. 10. The twenty-five levels of excitation that are shown are all separated by the photon energy. Most of the levels do not have enough energy to dissociate. However, all levels above the barrier height to isomerization do decay through one or both of the product channels. The relative yield into the two reaction channels for each level is shown based on analysis similar to what has just been described. In the calculations of the RRKM rate constants, the theoretical Arrhenius A-factor of Dewar et. al.[23] was used for the isomerization reaction and an experimental A factor of $10^{15.6}$ was used for simple C-N bond rupture.[33] Fitting the data was done by adjusting the absorption cross sections in the QC so that the population distribution of dissociating molecules reproduced the observed translational energy release for reaction I. The results of the calculation of the $P(E_T)$ using RRKM theory is the solid line in fig. 2. Then, by varying the barrier height to isomerization, keeping the A-factor constant, we fit the observed branching ratio for the

two reactions. By this analysis the observed branching ratio of reaction II to reaction I of 0.6 led to a barrier height to isomerization of 55.5 kcal/mol. The substantially larger release of translational energy for reaction II compared to reaction I is also in good agreement with that expected from RRKM theory based on the internal energy distribution that the isomerization yield curve in fig. 10 predicts.

From the description so far one might suspect that the inherent error in such an analysis would be too large to obtain any useful results. In fact this is not the case. Although the absorption cross sections for states in the QC can vary by more than a factor of three ($0.08 \times 10^{-19} cm^2$ to $3.0 \times 10^{-19} cm^2$) within the constraints of the observed translational energy release of the simple bond rupture reaction, this gives rise to only a $\pm$ 1.5 kcal/mol uncertainty in the barrier height to isomerization.

The major sources of error in the derivation of the barrier height are the uncertainty associated with the Arrhenius A-factor used for isomerization and the uncertainty in the measured branching ratio due to the low signal to noise ratio in this experiment. Fortunately, the calculation of the barrier height is not very sensitive to error in the A-factor. We found that if the A-factor is off by a factor of 3, it only changes the barrier height by 3 kcal/mol.

There are some questions that still remain concerning the branching ratio measurement. If it is true that 41 percent of the fast contribution to mass 30 is NO^+ this means that the mass spectrum for methoxy radical consists of mass 29 (HCO^+) and mass 30 (H_2CO^+) with the intensity

ratio being 1:4 in favour of H_2CO^+. On the basis of the thermodynamics alone it is surprising that H_2CO^+ outweighs HCO^+ by four to one and not the other way around. If the value of .41 were in error, the most drastic effect on the branching ratio would be if all of the fast contribution to the mass 30 TOF spectrum were NO^+. Then the branching ratio would be 1.5 in favor of isomerization. Although this is quite a large change in the branching ratio, the consequent change in the barrier height is only 1.5 kcal/mol, from 55.5 kcal/mol to 54.0 kcal/mol.

There is yet another experimental uncertainty due to the poor signal to noise ratio of the data which causes fairly large uncertainty in the translational energy release of the decomposing methylnitrite, symbolized by the cross-hatched area in fig. 3. The branching ratio of 0.6 is based on the results of the RRKM calculation of the translational energy release shown as the thick line in fig. 3. This is clearly on the slow side of the indicated error bars. If the true translational energy release of the products were given by the fastest edge of the error bars in fig. 3, this would have the effect of raising the relative contribution of reaction II in the c.m. frame. This effect alone would change the branching ratio from 0.6 to 1.2 and would lower the barrier height by another 1.0 kcal/mol.

It should be noted that this is quite a conservative estimation of the error, since it is very unlikely, if RRKM theory accurately reflects the release of translational energy in methylnitrite, that there could possibly be as large a release of translational energy as the fast edge of the error bars in fig. 3 reflect. Using the A factor for simple bond rupture of methylnitrite of $10^{15.6}$,[34] this large a release of translational

energy would imply an average amount of excitation above the dissociation limit of 35 kcal/mol which is clearly unreasonable considering fig 10. If the average level of excitation were 35 kcal/mol above CH_3O + NO, it would be 22 kcal/mol above the threshold for C-N bond rupture. The RRKM lifetime for C-N bond rupture at this degree of excitation is about 30 psec. It would therefore be impossible to pump CH_3NO_2 this high under our experimental conditions which give an average rate of photon absorption of 10^9/sec.

Finally, if all of the experimental uncertainties were to conspire in the most unfortunate way, so that all of the individual errors added to make the barrier height the lowest it could possibly be, it would change from the reported value of 55.5 kcal/mol to 51.5 kcal/mol. The analysis of the error in the barrier height determination is summarized in table V.

B. THE EXIT BARRIER FOR HONO ELIMINATION FROM $C_2H_5NO_2$ AND $2\text{-}C_3H_7NO_2$

The best test of the branching ratio matching method for the barrier height determination for isomerization of nitromethane is to apply it to an analogous system where the value of the barrier height is already known. Nitroethane is ideal since the Arrhenius A-factor and activation energy for reaction IV are well known experimentally.[28] The A-factor for reaction III is assumed to be the same as for reaction I. The approach was to use the measured translational energy release distribution for reaction III as a "thermometer" for the internal energy distribution of the dissociating molecules. By varying the absorption cross sections in the QC to reproduce

this data (solid line in fig. 5) and adjusting the barrier height for HONO elimination (reaction IV) to match the observed branching ratio, we arrived at a value of 46 ± 1.5 kcal/mol for the barrier height to HONO elimination from $C_2H_5NO_2$.

Fig. 11 shows a schematic representation of this calculation which is similar to the nitromethane calculation. The only difference is that now we cannot use the translational energy distribution of reaction IV to double check the calculation since RRKM theory cannot predict the product energy distribution for molecular elimination reactions. One advantage of the large translational energy release in the molecular elimination channel is that we can fully resolve the two proccesses in the TOF spectra and therefore there is much less uncertainty in the measured branching ratio. This reduces the error in the determination of the barrier height of the HONO elimination reaction. Consequently, the major source of error is in the determination of the translational energy release of the simple bond rupture reaction which leads to the stated uncertainty.

In order to compare this to the experimental activation energy, we must make use of equation (3) which relates the activation energy at a specific temperature to the height of the barrier.

$$E_a = \frac{\sum \epsilon_i k_i g_i e^{-\epsilon_i/kT}}{\sum k_i g_i e^{-\epsilon_i/kT}} - \left\{ - \frac{\delta \ln Q}{\delta (1/T)} \right\} \qquad (3)$$

where:

ϵ_i = energy of the i^{th} level

k_i = rate constant for dissociation of the i^{th} level

g_i = degeneracy of the i^{th} state

k = Boltzmann's constant

T = Temperature of pyrolysis experiment

Q = Molecular partition function excluding translation

The density of states as a function of total energy was used to approximate the g_i's above, the k_i's are derived from RRKM theory, and the summation was carried out numerically. The activation energy obtained is 45 ± 1.5 kcal/mol at 700°K, in excellent agreement with the experimental result of 45 kcal/mol.[28] This is the most direct test of our method of determining barrier heights in two channel dissociation systems and leads us to believe it is quite reliable.

Although there is significant scatter in the data, it does appear that the average translational energy release for HONO elimination from 2-nitropropane is slightly less than for nitroethane by about 3-5 kcal/mol. In the abscence of good thermochemical and kinetic data we applied our method of branching ratio matching in order to see if there was any reason to believe that the barrier height to HONO elimination was lower in 2-nitropropane than in nitroethane. Of course, one must make certain assumptions. First of all, in order to get an absolute value for the barrier height, we must know the simple bond rupture endothermicities. From ref. 34, the ΔH_{298}'s of reactions I, III and V are 60.0, 57.7 and 59.7

kcal/mol, respectively. We do expect that the C-N bond energies of the series nitromethane, nitroethane, and 2-nitropropane should decrease, due to the increasing stabilization of the free radical. Indeed, this can be seen in the C-H bond energies of methane, ethane and propane (to form isopropyl radical and H).[35] In that series a stabilization of ~3kcal/mol is obtained by adding each methyl group. It is immediately apparent that the 59.7 kcal/mol value for 2-nitropropane is suspect since it is nearly as strong as nitromethane. For this reason we have assumed the C-N bond energies in the series to be 59.4, 56.4 and 53.4 kcal/mol respectively. This includes a small (~0.5 kcal/mol) correction from ΔH_{298} to D_o(C-N) and conforms to the expected trend.

The A-factor for the simple bond rupture of nitromethane is well known to be $10^{15.6}$.[33] Since the extra degrees of freedom present in nitroethane and 2-nitropropane are not expected to play an important role in the simple bond rupture reactions of these molecules, it is reasonable to assume that the A factors for reactions I, III, and V are the same.

The A factor for the HONO elimination from 2-nitropropane was assumed to be a factor of two larger than the recommended value for HONO elimination from nitroethane. This is a simple result of the reaction path degeneracy of the two reactions and can be understood by realizing that there are twice as many H atoms that can undergo transfer to the NO_2 moiety and subsequent HONO elimination in 2-nitropropane than there are in nitroethane.

The final assumption that has been made in the comparison of 2-nitropropane to nitroethane is that the endothermicities of the HONO elimination channels are the same. Experimentally they differ by two

kcal/mol, but the error in these values is large enough to make it impossible to state that they are in fact different. For the purpose of comparison, the assumption of equality is preferred to the experimental values because the difference in experimental endothermicities contradicts the reasonable expectation that the HONO elimination from 2-nitropropane should be slightly less endothermic than that from nitroethane if, in fact, there were to be any difference at all.[36] The prefered thermochemical and kinetic values, both experimentally determined and assumed, for all of the systems we have studied are summarized in table VI.

The application of the branching ratio matching method is done in exactly the same way as before. This procedure yields a barrier height of 41 kcal/mol, a full 5 kcal/mol lower than in nitroethane. There is one inconsistency in this calculation in that the calculated best fit (solid line of fig. 7) requires the absorption cross sections in the QC to be 1.0×10^{-19} cm^2. This is to be compared to the values for nitromethane and nitroethane of 0.15×10^{19} cm^2 and 0.20×10^{-19} cm^2, respectively. While it is possible that this is a real effect, if the true value of the absorption cross sections in 2-nitropropane were to be more in line with nitromethane and nitroethane, say 0.25×10^{-19} cm^2, the calculated translational energy release for the simple bond rupture reaction would still agree fairly well with the data as shown in fig. 8 (dashed curve) and the barrier height would then be 43 kcal/mol. This would lead to the same conclusion that the barrier height to HONO elimination is somewhat lower in 2-nitropropane than in nitroethane.

One interesting phenomenon in the IRMPD of nitroethane and 2-nitropropane is the absence of evidence for the unimolecular isomerization and formation of alkoxy radicals and NO, for example reaction VII.

$$C_2H_5NO_2 \longrightarrow \overset{\ddagger}{C_2H_5ONO} \longrightarrow C_2H_5O + NO \qquad \text{(VII)}$$

This can be understood by considering the competition between HONO elimination and isomerization in an analagous way to the calculations represented by figures 10 and 11. We used the known A-factor and barrier height for HONO elimination for reaction IV and the same barrier height and A-factor for the isomerization of nitromethane to characterize reaction VII. Then by using the same absorption cross sections as in the calculation represented by fig. 11, we obtained a branching ratio of more than 10:1 in favour of HONO elimination. This, at first glance, may seem odd since we know that the isomerization channel can compete with simple bond rupture in nitromethane. However, an inspection of fig. 10 reveals that in nitromethane the isomerization channel competes only because it can dissociate from levels below the dissociation limit of the simple bond rupture channel, or at sufficiently low energies that the rate constant for simple bond rupture is quite small. As soon as the system has an internal energy of about 6 kcal/mol above the C-N bond energy, simple bond rupture dominates. In nitroethane, in order for isomerization to be important there must be no other reactions that can dissociate rapidly from the energy levels below or near the energy threshold for simple bond rupture. Since the HONO elimination channel is present this cannot be the case. The same is true in the dissociation of nitropropane and explains the absence of the isomerization channel.

C. THE TRANSLATIONAL ENERGY RELEASE IN CONCERTED MOLECULAR ELIMINATION REACTIONS: $C_2H_5NO_2$ AND 2-$C_3H_7NO_2$

For a reaction that goes over a substantial mechanical barrier in the PES, the essential question we must address is what is the nature of the potential energy barrier and to what extent does the potential energy of that barrier appear as product translation. For instance, in the concerted four-center elimination of HCl from 1,1,1-trichloroethane, the transition state is a very distorted configuration, far from the equilibrium structure of the products or the reactant. Consequently, when the electrons rearrange to form products, the potential energy of the barrier will appear mainly as internal energy of the products as the molecules make their way back to their equilibrium configurations, and only a relatively small fraction of the potential energy of the exit barrier appears as translation.[37] On the other hand, in the dissociaton of formaldehyde to H_2+CO, the transition state corresponds to a configuration in which one of the hydrogens moves toward the other hydrogen without extending the CO or CH bonds. The formation of the H_2 bond takes place at close proximity to the CO. The potential energy in this case mainly appears as repulsion between H_2 and CO and it is not surprising that as much as 75 percent of the barrier appears as translation.

In the case of nitroethane or 2-nitropropane, the transition state of the reaction at the top of the mechanical barrier in the PES is a five membered ring. With the exception of the transfer of H from C to O, it is not necessary to distort the molecule very far from its equilibrium bond lengths and angles to reach the five membered ring transition state. This

implies that the potential energy barrier is mainly due to repulsion of the closed shell products after the electrons have rearranged to the configuration of the products and not to "strain energy" of the reactant molecule. We recognize that this is similar to CH_2O and are therefore not surprised to see an average release of translational energy of 20 kcal/mol, 70 percent of the 28 kcal/mol exit barrier.

For the case of 2-$C_3H_7NO_2$ we see an average release of translational energy of 15 kcal/mol or 65 percent of the 23 kcal/mol exit barrier. A comparison of the two systems implies that there is more involved here than just a difference in the barrier heights since the fraction of energy appearing as translation is different. Since it is clear that strain energy is relatively unimportant in producing the mechanical barrier in the PES's of these molecules, the difference must arise from the difference in the repulsive internal excitation dynamics as the fragments descend down the barrier.

We have used a "scaled-reduced-mass impulse approximation" to interpret the differences between nitroethane and 2-nitropropane in the translational energy release of the concerted molecular elimination channels. To calculate the relative amounts of translational and internal energy in the products using the standard impulse approximation for the case when C and N are initially only very loosely coupled to the rest of the atoms, one assumes that the impulsive energy release is sufficiently sudden that momentum is initially balanced between the two repulsive sites, the C and N atoms and all the other atoms are spectators, as shown in equations (4).

$$m_C v_C = m_N v_N$$
$$m_C E_C = m_N E_N \qquad (4)$$

This means that, initially, the total available energy all appears as the kinetic energy of C and N atoms, $E_C + E_N$. The final translational energy release for nitroethane must also balance linear momentum between HONO and C_2H_4 according to equations (5),

$$\begin{aligned} {}^{m}C_2H_4{}^{v}C_2H_4 &= {}^{m}HONO{}^{v}HONO \\ {}^{m}C_2H_4{}^{T}C_2H_4 &= {}^{m}HONO{}^{T}HONO \end{aligned} \qquad (5)$$

and the total final translational energy would be $T_{HONO} + T_{C_2H_4}$. The difference between the total available energy ($E_C + E_N$) and the total translational energy ($T_{HONO} + T_{C_2H_4}$) is the amount of internal excitation due to the relative motion between the C and N atoms and the atoms they are bound to. If one works through this calculation one comes up with 0.4 of the available energy or barrier height appearing as translation. This low value clearly indicates that the infinitely loose limit of this approximation is not realistic. In contrast, the infinitely rigid limit of this approximation would neglect all product vibrational degrees of freedom and simply require the balance of linear and angular momentum between HONO and C_2H_4. One would then predict that nearly all of the available energy would appear as translation of the products. Apparently, the true situation lies somewhere in between. A convenient way to scale the extent of coupling between C and N atoms and the atoms they are bound to is by way of the effective reduced mass in the impulse approximation. One can see that in the infinitely loose limit, the reduced mass of the impulse aproximation is simply the reduced mass of the C,N pair or μ_{min}=6.46. The reduced mass for the infinitely rigid limit would be

that of the HONO,C_2H_4 pair or μ_{max}=17.55. There will be an effective reduced mass between these two that predicts the observed amount of translational energy release. In order to reproduce the experimentally observed translational energy release of 0.7 of the exit barrier, it is neccesary to have an effective reduced mass of μ_{eff}=12.5 which is about twice as large as the reduced mass of C and N or 70 percent of the reduced mass of C_2H_4 and HONO. We can define an empirical parameter α by equation (6).

$$\alpha = (\mu_{eff} - \mu_{min})/(\mu_{max} - \mu_{min}) \qquad (6)$$

α is reflective of the deviation from each limit of the approximation. The interesting thing about α is that if one repeats the analysis just descibed for the case of 2-nitropropane, assuming α to be the same in 2-nitropropane as in nitroethane, one arrives at 0.66 of the exit barrier potential energy going into translation, in very good agreement with experiment. To get an idea of the general usefulness of this method consider table VII. For UV photodissociation of alkylhalides the principle mechanism of product internal excitation is also repulsive excitation. By setting α=0.44 we were able to obtain very good agreement between the model and the experimental results for 5 different molecules. In addition, it is also clear that the dissociation of C_2F_4BrI at 193 nm is anomolous. This might be due to another mechanism besides direct repulsive excitation as was hypotheosized by Krajnovich et. al.[38] Since at 193 nm the excitation is an $n(Br)\rightarrow\sigma^*(C-Br)$ transition, electronic energy transfer to the C-I bond must precede C-I bond rupture.

V. CONCLUSIONS

The major conclusion of this work is that it is possible to make a quantitative connection between molecular beam IRMPD experiments and classical thermolysis experiments. This is accomplished through the use of RRKM theory and relies on the relationship between the translational energy distribution for simple bond rupture reactions and the internal energy distribution of the ensemble of dissociating molecules. Due to the unambiguous determination of and discrimination between different primary unimolecular decomposition pathways, the molecular beam IRMPD experiments can provide information on the energetics and dynamics of a system where pyrolysis techniques would be mired in an overly complex set of primary and secondary dissociation proccesses. Yet it is also possible to use this technique, where the concept of temperature is meaningless, to predict phenomenolgical quantities such as activation energies that are normally measured under collisional, thermal conditions.

Specifically, we have been able to observe the isomerization of nitromethane to methylnitrite and make a good estimation of the isomerization barrier height using a branching ratio matching method. We have tested this method by using it to determine the barrier height and activation energy to HONO elimination from nitroethane and find excellent agreement with the known activation energy. We then used the same procedure to determine the barrier height for HONO elimination from 2-nitropropane and have found that there is good reason to believe that this barrier height is 3-5 kcal/mol lower than in nitroethane.

We have also observed very large releases of translational energy in concerted molecular elimination reactions of nitroalkanes which proceed through 5 membered cyclic transition states. We have used a scaled reduced mass impulse approximation to interpret the difference in translational energy release between 2-nitropropane and nitroethane. Within a "family" of dissociating molecules we have found that this model can be used to predict the relative translational energy release from one member to another when impulsive internal excitation is the principle mechanism of product internal excitation. We have suggested that this large translational energy release is due to the formation of products near their equilibrium geometries in very close proximity to one another. We expect that this will be a general feature of concerted molecular elimination reactions that proceed through a cyclic transition state that can be formed without a great deal of molecular distortion.

ACKNOWLEDGEMENT

This work was supported by the Office of Naval Research under contract No. N00014-83-K-0069

REFERENCES

1. N.R. Isenor, M.C. Richardson, Appl. Phys. Lett., 18, 224 (1971)

2. N.R. Isenor, M.C. Richardson, Optics Commun., 3, 360 (1971)

3. V.S. Letokhov, E.A. Ryabov, O.A. Tumanov, Optics Commun., 5, 168 (1972)

4. V.S. Letokhov, E.A. Ryabov, O.A. Tumanov, Sov. Phys. J.E.T.P. (Engl. transl.), 36, 1069 (1973)

5. N.R. Isenor, V. Merchant, R.S. Halworth, M.C. Richardson, Can. J. Phys., 51, 1281 (1973)

6. R.V. Ambartzumian, Yu.A. Gorokov, V.S. Letokhov, G.N. Makarov, J.E.T.P. Lett. (Engl. transl.), 21, 171 (1974)

7. R.V. Ambartzumian, Yu.A. Gorokov, V.S. Letokhov, G.N. Makarov, J.E.T.P. Lett. (Engl. transl.), 43, 22 (1975)

8. J.L. Lyman, R.J. Jensen, J. Rink, C.P. Robinson, S.D. Rockwood, Appl. Phys. Lett., 27, 87 (1975)

9. See for example: N. Bloembergen, E. Yablonovitch, Physics Today, pp. 23-30, May (1978); M.N.R. Ashfold, G. Hancock, Gas Kinetics and Energy Transfer, Royal Soc. (Spec. Per. Rep.), 4, pp. 73-116 (1980); C.D. Cantrell, S.M. Freund, J.L. Lyman, The Laser Handbook, North Holland Pub. Co., M.L. Stitch Ed., pp. 485-576 (1979); P.A. Schultz, Aa.S. Sudbo, D.J. Krajnovich, H.S. Kwok, Y.R. Shen, Y.T. Lee, Ann. Rev. Phys. Chem., 30, 379 (1979)

10. J.D. Rynbrandt, B.S. Rabinovitch, J. Phys. Chem., 75, 2164 (1971)

11. J.P. Maier, A. Seilmeier, A. Laubereau, W. Kaiser, Chem. Phys. Lett., 46, 527 (1977)

12. P.J. Robinson, K.A. Holbrook, Unimolecular Reactions, John Wiley and Sons Pub. Co., London (1972)

13. M.J. Coggiola, P.A. Schultz, Y.T. Lee, Y.R. Shen, Phys. Rev. Lett., 38, 17 (1977)

14. E.R. Grant, M.J. Coggiola, Y.T. Lee, P.A. Schultz, Aa.S. Sudbo, Y.R. Shen, Chem. Phys. Lett., 52, 595 (1977)

15. Aa.S. Sudbo, P.A. Schultz, E.R. Grant, Y.R. Shen, Y.T. Lee, J. Chem. Phys., 68, 1306 (1978)

16. Aa.S. Sudbo, P.A. Schultz, E.R. Grant, Y.R. Shen, Y.T. Lee, J. Chem. Phys., 70, 912 (1979)

17. L.J. Butler, R.J. Buss, R.J. Brudzynski, Y.T. Lee, J. Phys. Chem., 87, 5106 (1983)

18. F. Huisken, D. Krajnovich, Z. Zhang, Y.R. Shen, Y.T. Lee, J. Chem. Phys., 78, 3806 (1983)

19. E.R. Grant, P.A. Schultz, Aa.S. Sudbo, Y.R Shen, Y.T. Lee, Phys. Rev. Lett., 40, 115 (1978)

20. The problem of using RRKM theory to calculate the product energy distributions for reactions with exit barriers has received considerable attention. See for example: R.A. Marcus, J. Chem. Phys., 62, 1372 (1975) and G. Worry, R.A. Marcus, J. Chem. Phys., 67, 162 (1977), however one must always make dynamical assumptions in such theories.

21. A.M. Wodtke, E.J. Hintsa, Y.T. Lee, J. Chem. Phys., 84, 1044 (1986)

22. B.H. Rockney, E.R. Grant, J. Chem. Phys., 79, 708 (1983)

23. M.J.S. Dewar, J.P. Ritchie, J. Alster, J. Org. Chem. 50, 1031 (1985)

24. R.J. Bartlett has performed ab initio calculations placing an upper bound to the barrier height to isomerization in nitromethane at 70 kcal/mol.

25. A.M. Wodtke, Y.T. Lee, J. Phys. Chem., 89, 4744 (1985)

26. D.A. Dixon, A. Komornicki, W.P. Kraemer, J. Chem. Phys., 81, 3603 (1984) give heats of formation for H_2COH^+ and HCO^+ of 165.2 and 197.9 kcal/mol respectively. The relative instability H_3CO^+ with respect to H_2COH^+ is estimated to be 80 kcal/mol based on the 107 kcal/mol O-H bond strength in H_2COH^+ and assuming that the C-H bond strength in H_3CO^+ is 27 kcal/mol, the same as in H_2CO^+. This gives an exothermicity for H_2 elimination from H_3CO^+ of 47 kcal/mol.

27. R.E Center, A. Mandl, J. Chem. Phys., 57, 4104 (1972) Atomic polarizabilities can be found in T.M. Miller, B. Bederson, Adv. At. Mol. Phys., 13, 1 (1977). Molecular polarizabilities are assumed to be the sum of the constituent atomic polarizabilities.

28. G.N. Spokes, S.W. Benson, J. Am. Chem. Soc., 89, 6030 (1967)

29. The electron impact ionization mass spectrum of CH_3ONO consists of m/e = 46:30:61 abundances of 1:100:0 at an electron energy of 250 eV. Our electron energy was 200 eV. Atlas of Mass Spectral Data, 1, p. 41, E. Stenhagen, S. Abrahamson, F.W. McLafferty Eds., John Wiley and Sons Pub. Co., New York (1969)

30. S.A Safron, N.D. Weinstein, D.R. Herschbach, J.C. Tully, Chem. Phys. Lett., 12, 564 (1972)

31. This program has been reported earlier: P.A. Schultz, Aa.S. Sudbo, E.R. Grant, Y.R. Shen, Y.T. Lee, J. Chem. Phys., 72, 4985 (1980) and is an extension of previous work by J.L. Lyman, J. Chem. Phys., 67, 1868 (1977) and W. Fuss, Chem. Phys., 36, 135 (1979)

32. D.J. Krajnovich, Ph.D. Thesis, pp. 83-90, University of California, Berkeley (1983)

33. L. Phillips, R. Shaw, Tenth Int. Symp. on Comb., p. 453 (1964) and V. Yashtern, Chemical Kinetics and Chain Reactions, 286, p. 313, U.S.S.R. Acadamy of Sciences, Moscow (1966)

34. S.W. Benson, H.E. O'Neal, Kinetic Data on Gas Phase Unimolecular Reactions, National Standard Reference Data Series, National Bureau of Standards (1970), Library of Congress Card Catalog ∝68-67395

35. See the very accurate theoretical work of C.F. Melius, J.S. Binkley, M.L. Kszykowski, Proc. Combustion Res. Contractors Meeting, May (1984), U.S. Dept. of Energy, Office of Energy Sciences, for calculations of the heats of formation for CH_3, C_2H_5, and $2\text{-}C_3H_7$.

36. C.F. Melius, J.S. Binkley, M.L. Kszykowski, Proc. Combustion Res. Contractors Meeting, May (1984), U.S. Dept. of Energy, Office of Energy Sciences. Consider the analogous H_2 elimination from ethane and n-propane in view of Melius' calculation of heats of formation for C_2H_6, C_2H_4, C_3H_8 and C_3H_6.

37. Aa.S. Sudbo, P.A. Schultz, Y.R. Shen, Y.T.Lee, J. Chem. Phys., 69, 2312 (1978)

38. D. Krajnovich, L.J. Butler, Y.T. Lee, J. Chem. Phys., 81, 3031 (1984)

39. G.N.A. Van Veen, Excited Species from Photofragmentation, Ch. 8, Proefschrift, Stichtung voor Fundamenteel Onderzoek der Materie (Foundation for Fundamental Research on Matter), Amsterdam, the Netherlands

40. R.K. Sparks, K. Shobatake, L.R. Carlson, Y.T. Lee, J. Chem. Phys., 75, 3838, (1981)

41. T.K. Minton, P. Felder, R.J. Brudzynski, Y.T. Lee, J. Chem. Phys., 81, 1759 (1984)

TABLE I

EXPERIMENTAL CONDITIONS OF

PARENT MOLECULAR BEAMS

PARENT MOLECULE	STAGNATION[a] TEMPERATURE	STAGNATION[b] PRESSURE	PERCENT PARENT[c] IN BEAM	NOMINAL[d] VELOCITY	$\frac{\Delta V}{V}$[e]
CH_3NO_2	308°C	140 torr	17	1.3×10^5	.22
$C_2H_5NO_2$	345°C	170 torr	13	1.4×10^5	.18
$2\text{-}C_3H_7NO_2$	358°C	200 torr	12	1.4×10^5	.17

a. Same as nozzle temperature.

b. Pressure immediately behind nozzle.

c. All molecules were seeded in Helium.

d. Units are cm/sec.

e. (full width at half maximum) ÷ (Nominal beam velocity).

TABLE II

IRMPD MASS SPECTRUM OF

CH_3NO_2

m/e	IDENTITY OF ION	PRODUCT DETECTED	SIGNAL[a] INTENSITY
46	NO_2^+	NO_2	0.05
15	CH_3^+	CH_3	0.14
30	NO^+	NO_2	0.11
30	NO^+	NO	0.06
30	CH_2O^+	CH_3O	0.08
29	HCO^+	CH_3O	0.02

a. units are (ion counts/laser shot)

TABLE III

IRMPD MASS SPECTRUM OF

$C_2H_5NO_2$

m/e	IDENTITY OF ION	PRODUCT DETECTED	SIGNAL[a] INTENSITY
46	NO_2^+	NO_2	0.03
30	NO^+	NO_2	0.14
30	NO^+	HONO	0.02
29	$C_2H_5^+$	C_2H_5	0.09
27	$C_2H_3^+$	C_2H_5	0.07
27	$C_2H_3^+$	C_2H_4	.002
26	$C_2H_2^+$	C_2H_5	0.07
26	$C_2H_2^+$	C_2H_4	0.01

a. Units are (ion counts/laser shot)

TABLE IV

IRMPD MASS SPECTRUM OF

$2\text{-}C_3H_7NO_2$

m/e	IDENTITY OF ION	PRODUCT DETECTED	SIGNAL INTENSITY
46	NO_2^+	NO_2	0.04
43	$C_3H_7^+$	C_3H_7	0.10
41	$C_3H_5^+$	C_3H_7	0.11
41	$C_3H_5^+$	C_3H_6	0.01
30	NO^+	NO_2	0.25
30	NO^+	HONO	0.06

a. Units are (ion counts/laser shot)

TABLE V

UNCERTAINTY IN BARRIER HEIGHT DETERMINATION

FOR THE ISOMERIZATION OF NITROMETHANE

55.5 kcal/mol MOST PROBABLE VALUE OF BARRIER HEIGHT CONSISTENT WITH AN ARRHENIUS A-FACTOR OF $10^{13.3}$

MAGNITUDE OF ERROR	SOURCE OF UNCERTAINTY
-1.5 kcal/mol	; translational energy release of C-N simple bond rupture reaction in nitromethane
-1.5 kcal/mol	; amount of mass thirty that is NO^+
-1.0 kcal/mol	; translational energy release of N-O simple bond rupture reaction in methylnitrite
+1.5 kcal.mol	;translational energy release of C-N simple bond rupture

51.5 kcal/mol MINIMUM BARRIER HEIGHT CONSISTENT WITH ARRHENIUS A-FACTOR OF $10^{13.3}$

57.0 kcal/mol MAXIMUM BARRIER HEIGHT CONSISTENT WITH ARRHENIUS A-FACTOR OF $10^{13.3}$

TABLE VI

ASSUMPTIONS AND REFERENCES

FOR PERTINENT

THERMOCHEMICAL AND KINETIC

VALUES

PARENT MOLECULE	PROCESS	BARRIER HEIGHT	ΔH_0	ARRHENIUS A-FACTOR	ACTIVATION ENERGY
CH_3NO_2	SBR[a]	59.4[b]	59.4[c]	15.6[d]	59[c]
CH_3NO_2	ISO[e]	55.5[f]	2.5[c]	13.3[g]	
CH_3ONO	SBR	41.0[b]	41.0[c]	15.6[d]	
$C_2H_5NO_2$	SBR	56.4	56.4[h]	15.6[i]	56[h]
$C_2H_5NO_2$	CME[j]	46.0[f]	18.0[c]	12.4[d]	45[f,k]
$2\text{-}C_3H_7NO_2$	SBR	53.4	53.4[h]	15.6[i]	53[h]
$2\text{-}C_3H_7NO_2$	CME	41.0[f]	18.0[l]	12.7[m]	40[f,n]

a. Simple bond rupture.

b. For SBR reaction no barrier to reverse reaction is assumed.

c. Units are kcal/mol, see ref. 34.

d. Units are logarithmic, see ref. 34.

e. Isomerization.

f. Derived from branching ratio matching analysis (see text).

g. See to ref. 23.

h. Based on 3 kcal/mol stabilization for each added methyl group, see text.

i. Assumed to be the same as for SBR of CH_3NO_2.

j. Concerted molecular elimination, HONO elimination.

k. Recommended experimental value, see ref. 28.

l. Assumed same as for nitroethane (see text).

m. Assumed to be twice the value of that for nitroethane (see text).

n. Experimental values range between 40 and 45 kcal/mol

TABLE VII

SCALED REDUCED MASS IMPULSE

APPROXIMATION ANALYSIS

REACTION	μ_{min}	μ_{max}	α	THEOR. E_T/E_a	OBS. E_T/E_a
IRMPD					
$C_2H_5NO_2 \longrightarrow C_2H_4+HONO$ [a]	6.46	17.55	.53	0.70	0.71
$C_3H_7NO_2 \longrightarrow C_3H_6+HONO$ [a]	6.46	22.18	.53	0.66	0.65
UV Excitation					
$CF_3I \xrightarrow{248\ nm} CF_3+I^*$ [b]	10.96	44.71	.44	0.58	0.61
$C_2F_5I \xrightarrow{248\ nm} C_2F_5+I^*$ [c]	10.96	61.43	.44	0.54	0.51
$CH_3 \xrightarrow{266\ nm} CH_3+I^*$ [d]	10.96	13.42	.44	0.90	0.88
$C_2H_4ClI \xrightarrow{266\ nm} C_2H_4Cl+I^*$ [e]	10.96	42.11	.44	0.59	0.58
$C_2F_4BrI \xrightarrow{248\ nm} C_2F_4Br+I^*$ [c]	10.96	74.63	.44	0.52	0.48
$C_2F_4BrI \xrightarrow{193\ nm} C_2F_4Br+I^*$ [c]	10.96	74.63	.44	0.52	0.37

a. This work.

b. See ref. 39.

c. See ref. 38.

d. See ref. 40.

e. See ref. 41.

FIGURE CAPTIONS

Fig. 1 TOF spectra from the IRMPD of nitromethane. The circles are the data and the solid lines are the fit to the data using the forward convolution method. Data was taken at 10° from the molecular beam. (a) NO_2 product from reaction I. (b) CH_3 product from reaction I. (c) NO_2 product from reaction I (---), NO as well as CH_3O product from reaction II (-·-·-). (d) CH_3O product from reaction II.

Fig. 2 Translational energy distribution of the products of reaction I. The cross-hatched area represents the uncertainty associated with the measurement and the solid line is the result of the model calculation described in section IV.A..

Fig. 3 Translational energy distribution of the products of reaction II. See caption of fig. 2.

Fig. 4 TOF spectra from the IRMPD of nitroethane. See caption of fig. 1. (a) NO_2 product of reaction III. (b) C_2H_5 product of reaction III. (c) NO_2 product of reaction III (---), HONO product of reaction IV (-·-·-). (d-e) C_2H_5 product of reaction III (---), C_2H_4 product of reaction IV (-·-·-).

Fig. 5 Translational energy distribution of the products of reaction III. See caption of fig. 2. Solid line is the result of the model calculation described in section IV.B..

Fig. 6 Translational energy distribution of the products of reaction IV. The cross hatching represents the uncertainty associated with the measurement and the solid line is the $P(E_T)$ which gives the best fit to the data.

Fig. 7 TOF spectra from the IRMPD of 2-nitropropane. See caption of fig. 1. (a) NO_2 product of reaction V. (b) C_3H_7 product of reaction V. (c) C_3H_7 product of reaction V (---), C_3H_6 product of reaction VI (-·-·-). (d) NO_2 product of reaction V (---), HONO product of reaction VI (-·-·-).

Fig. 8 Translational energy distribution of the products of reaction V. See caption of fig. 2. The dashed line is the result of the model calculation using absorption cross-sections in the QC of 0.25×10^{-19} cm^{-2} as described in section IV.B..

Fig. 9 Translational energy distribution of reaction VI. See caption of fig 6.

Fig. 10 Schematic representation of the model competition calculation for the unimolecular decomposition of nitromethane. The yield for the two dissociation pathways as a function of excitation energy is shown. See section IV.A..

Fig. 11 Schematic representation of the model competition calculation for the unimolecular decomposition of nitroethane. See caption of fig. 10 and section IV.B..

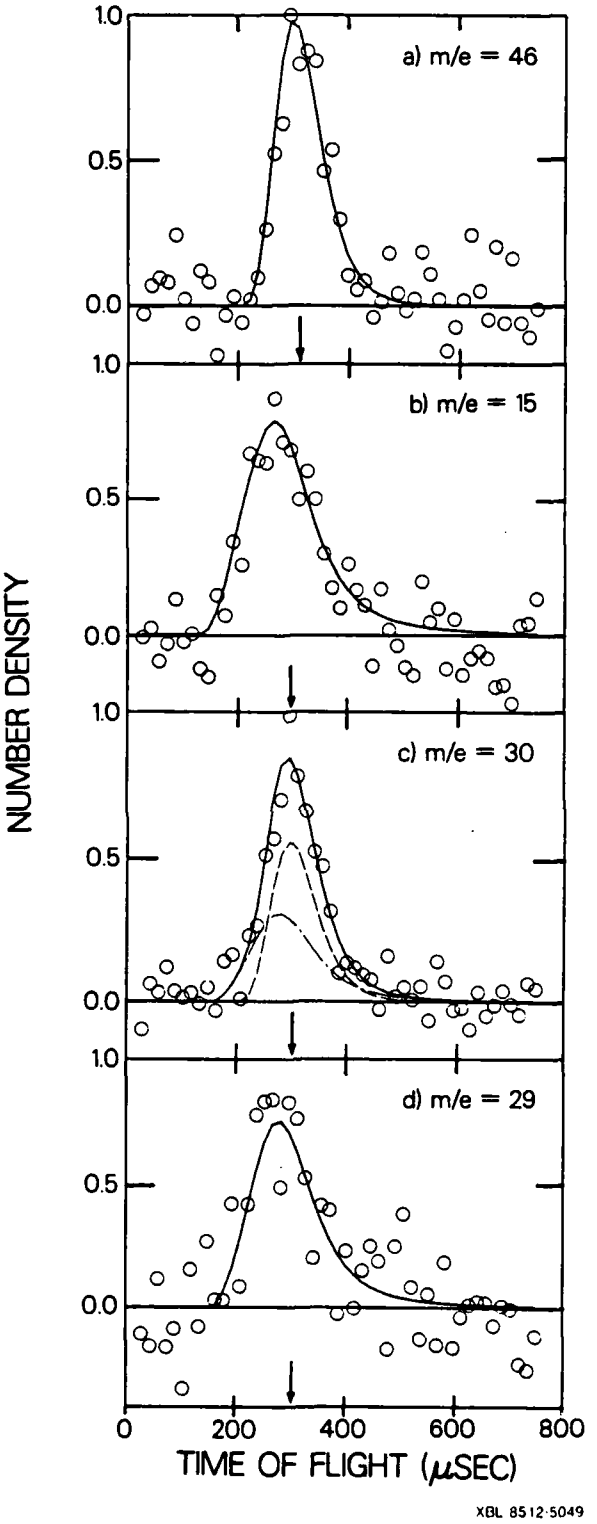
a) m/e = 46
b) m/e = 15
c) m/e = 30
d) m/e = 29
1.0
0.5
0.0
NUMBER DENSITY
0
200
400
600
800
TIME OF FLIGHT (μSEC)
XBL 8512-5049

Fig. 1

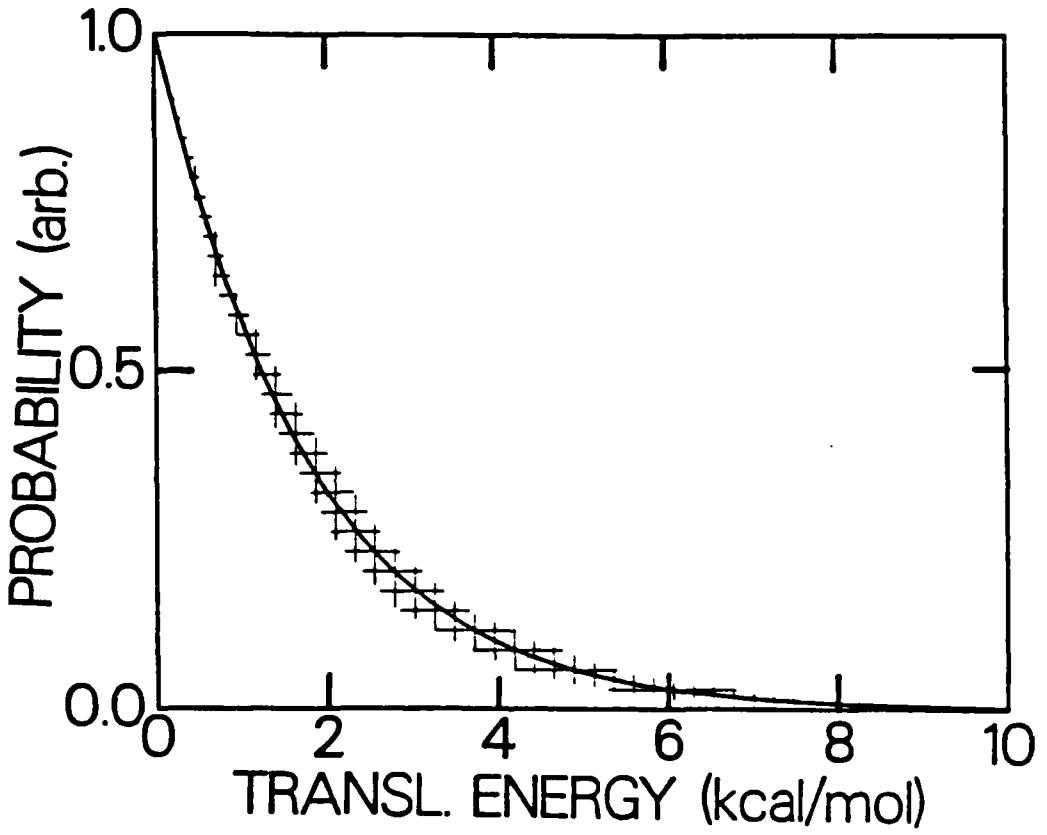

XBL 861-233

Fig. 2

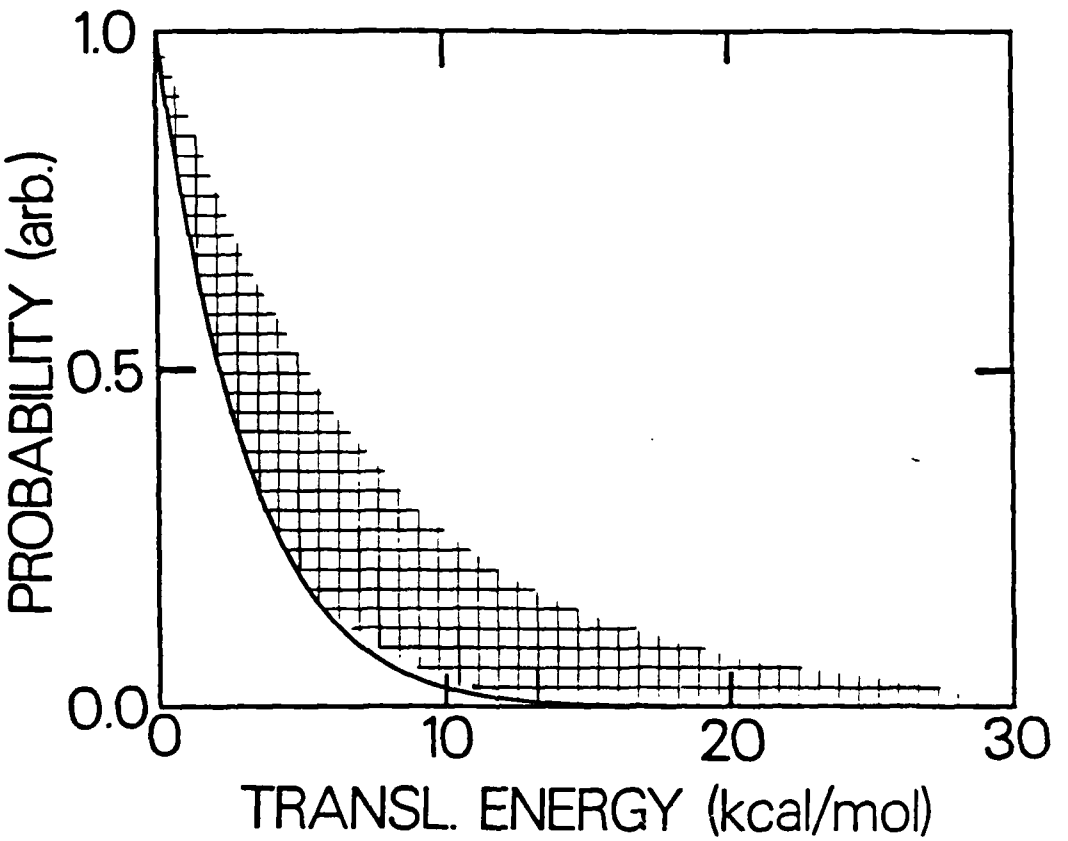

XBL 861-232

Fig. 3

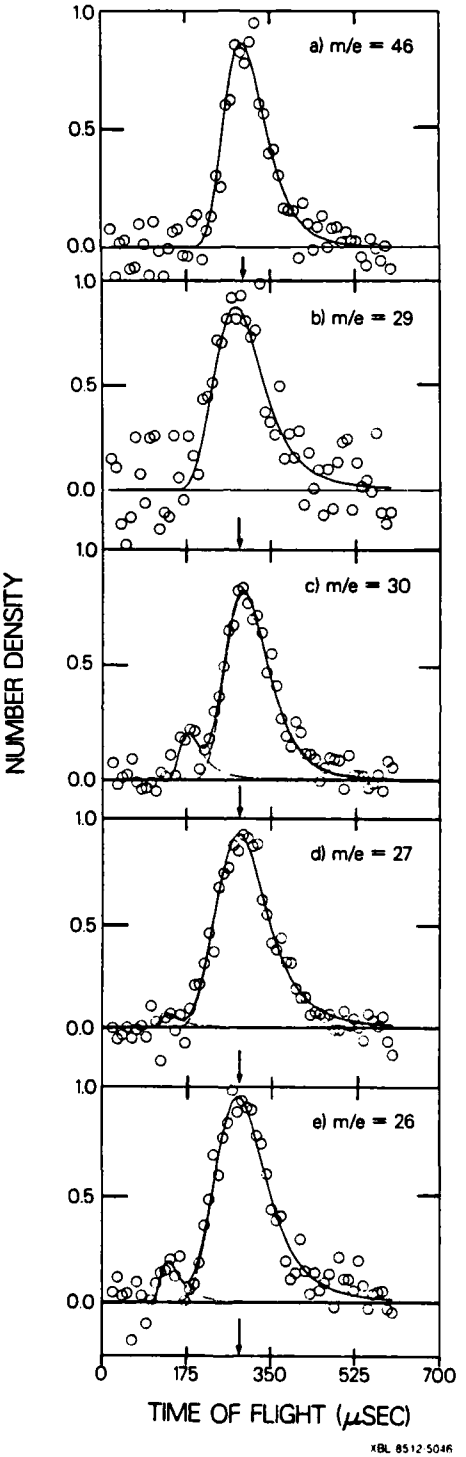
a) m/e = 46
b) m/e = 29
c) m/e = 30
d) m/e = 27
e) m/e = 26
1.0
0.5
0.0
NUMBER DENSITY
0
175
350
525
700
TIME OF FLIGHT (μSEC)
XBL 8512-5046

Fig. 4

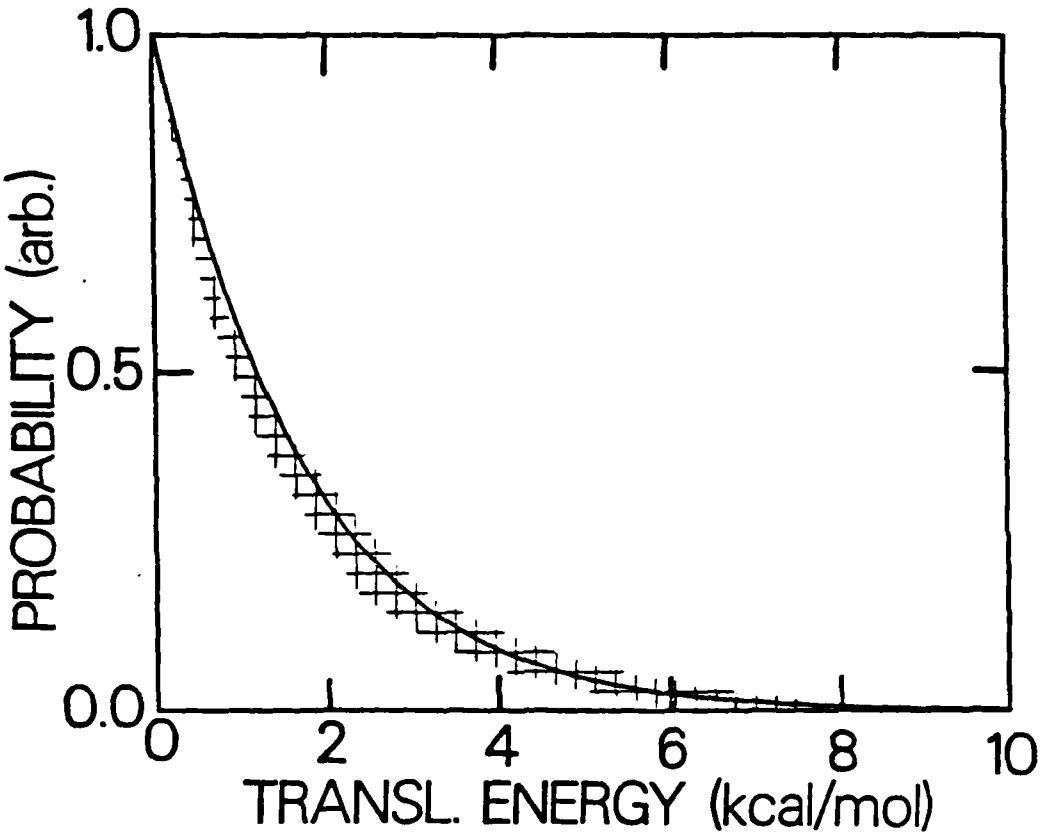

XBL 861-231

Fig. 5

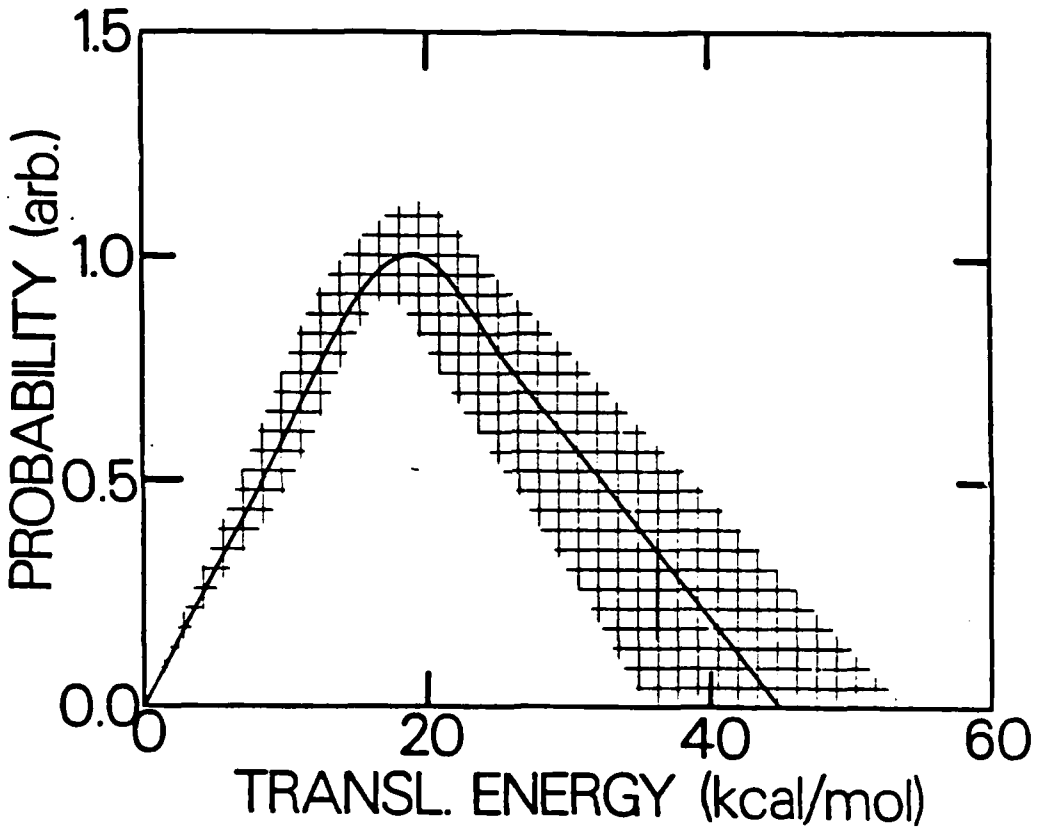

XBL 861-234

Fig. 6

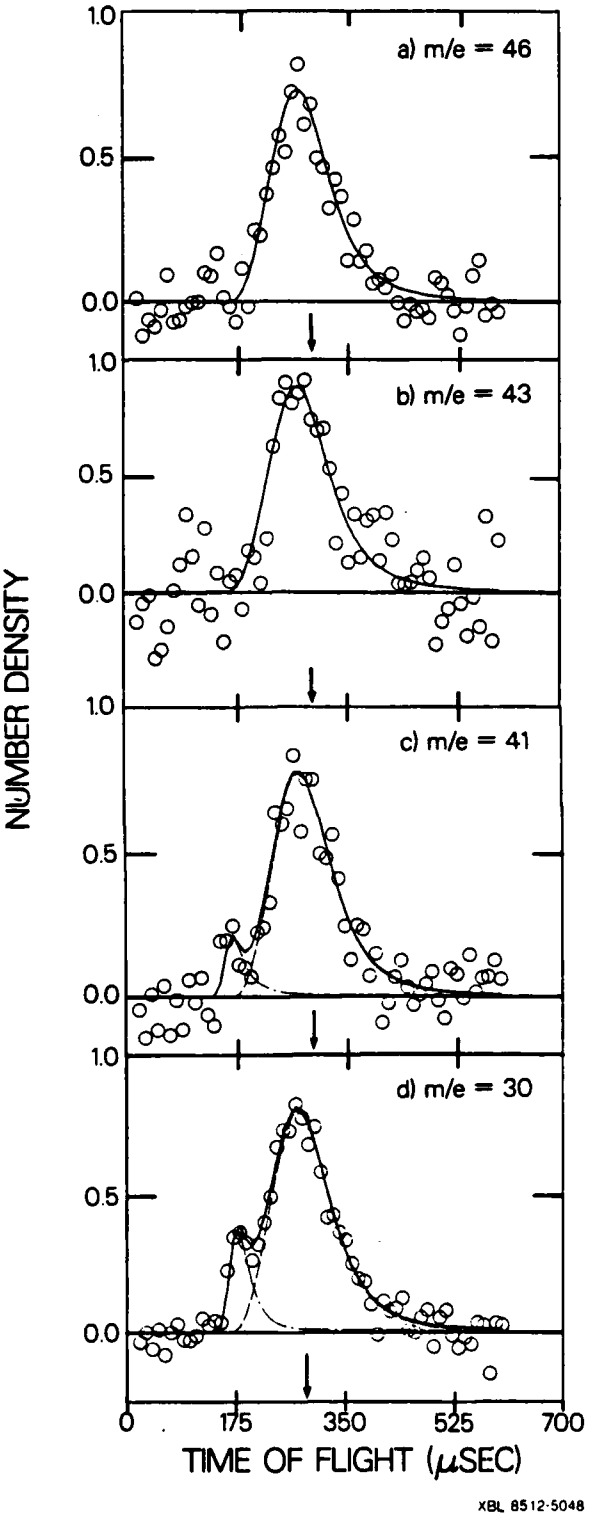
a) m/e = 46
b) m/e = 43
c) m/e = 41
d) m/e = 30
1.0
0.5
0.0
NUMBER DENSITY
0
175
350
525
700
TIME OF FLIGHT (μSEC)
XBL 8512-5048

Fig. 7

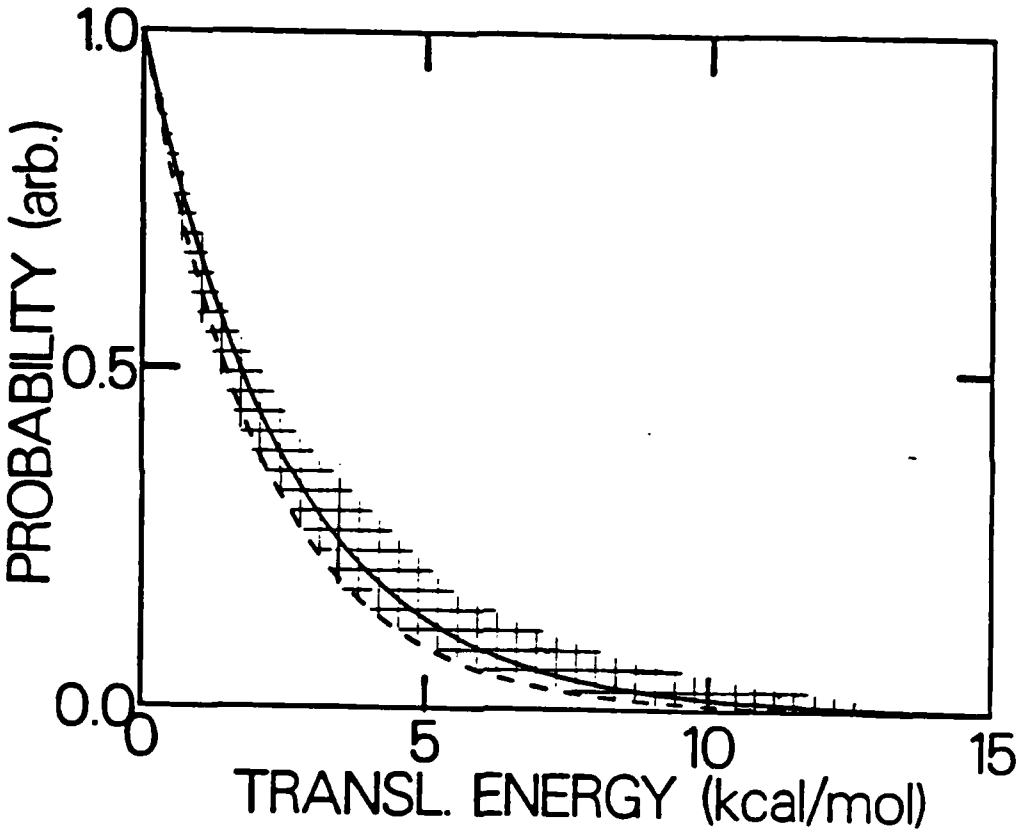

XBL 861-236

Fig. 8

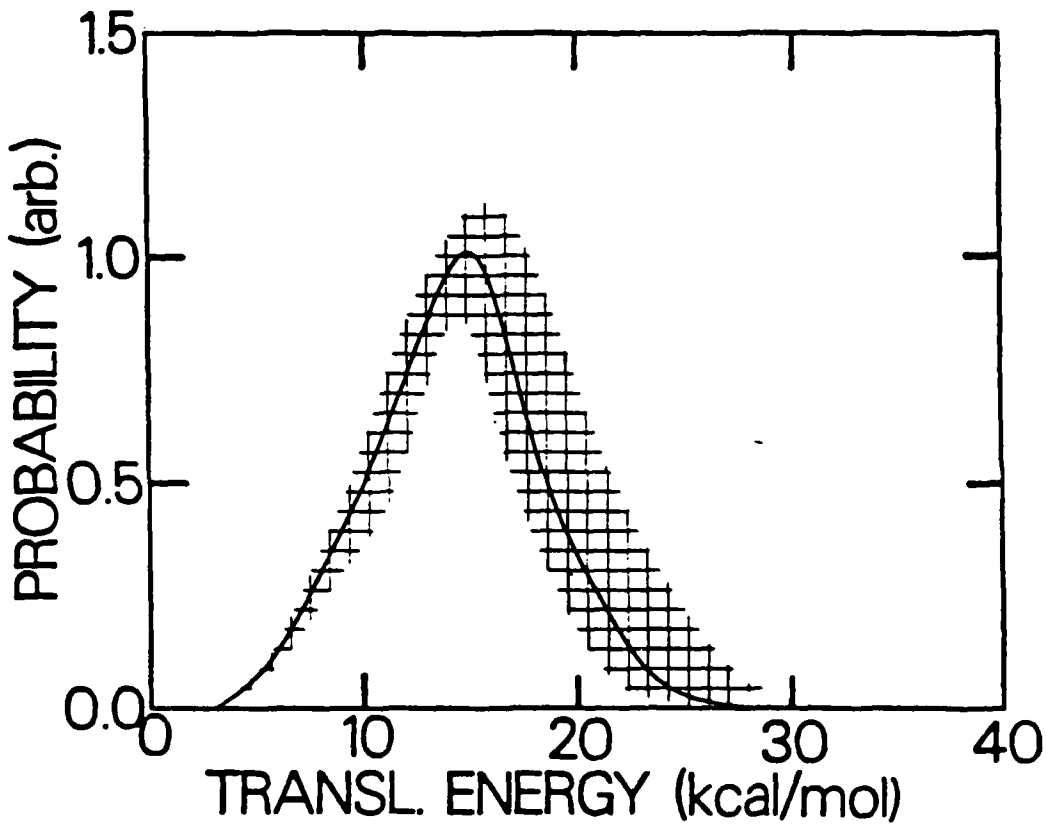

XBL 861-235

Fig. 9

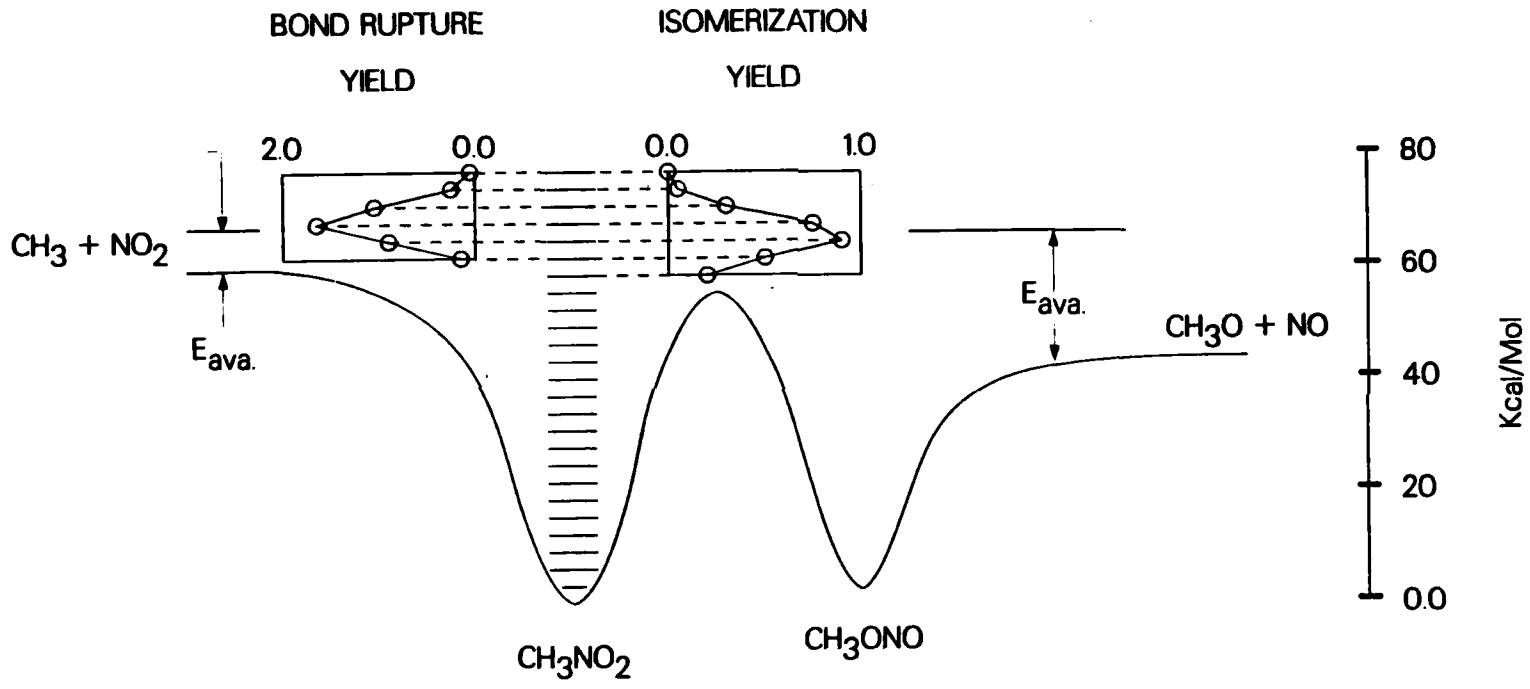
BOND RUPTURE
YIELD
ISOMERIZATION
YIELD
2.0
0.0
0.0
1.0
$CH_3 + NO_2$
$E_{ava.}$
$E_{ava.}$
$CH_3O + NO$
CH_3NO_2
CH_3ONO
80
60
40
20
0.0
Kcal/Mol
XBL 8512-5050

Fig. 10

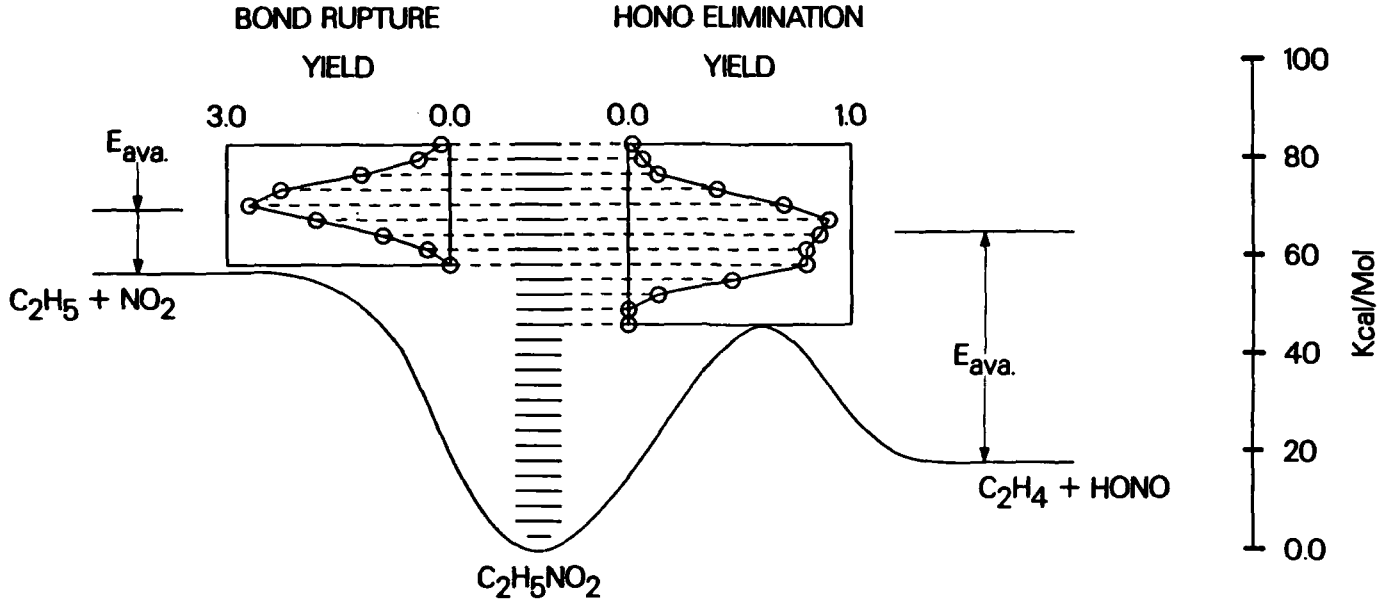
BOND RUPTURE
YIELD
3.0
0.0
HONO ELIMINATION
YIELD
0.0
1.0
$E_{ava.}$
$C_2H_5 + NO_2$
$C_2H_5NO_2$
$E_{ava.}$
$C_2H_4 + HONO$
100
80
60
40
20
0.0
Kcal/Mol
XBL 8512-5051

Fig. 11

DTIC

END

4-86